OBSERVATION OF INTRA-MACROPULSE POSITION MONITOR OF H⁻ BEAM OF CSNS LINAC*

C. Xie, Z. Xu, R. Qiu, C. Chen, M. A. Rehman, B. Zhang, R. Yang†
Institute of High Energy Physics, Beijing, China
also at Spallation Neutron Source Science Center, Dongguan, China

Abstract

The China Spallation Neutron Source (CSNS) accelerator, consisting of a H⁻ linac and a rapid cycling synchrotron (RCS), is undergoing an upgrade to increase the average beam power to 500 kW. At the CSNS linac, shorted-stripline beam position monitor (BPM) determines beam position by averaging over the entire macro-pulse. However, significant intra-macropulse beam position fluctuations have been observed in recent commissioning, which may cause undesired beam loss and degrade the injection efficiency. In this work, an intramacropulse beam position is reconstructed based on the signal integral algorithm. During 2025 autumn and 2026 spring operation, the intra-macropulse beam position behaviors have been uncovered at the MEBT and LRBT sections. Although beam conditions vary between two different experiments, a significant beam position drift during the first 100 μs, with a maximum amplitude of more than 5 mm, has been revealed.

POSITION RECONSTRUCTION ALGORITHM

The intra-macropulse beam position is reconstructed using a multi-step digital signal processing procedure. First, the raw BPM signals are digitally filtered to suppress noise and remove undesired frequency components. The processed signals are then segmented according to the chopper timing structure, where each segment corresponds to an individual chopped beam pulse with a repetition frequency of 1.02 MHz or 0.51 MHz. The normalized beam positions are subsequently calculated using the difference-over-sum method, followed by a third-order polynomial calibration derived from prior measurements to correct the position nonlinearity. By processing each segmented chopper window individually, the evolution of the intra-macropulse beam position within the macro-pulse can be reconstructed.

To investigate the influence of the sampling rate and filter bandwidth on the intra-macropulse beam position reconstruction, we using an R&S RTO2044 oscilloscope with a sampling rate of 6.25 GSPS and a vertical resolution of 16 bits to record data. In addition, a 20 kHz high-pass filter was applied to each electrode channel to suppress low-frequency interference from power supplies or magnet systems. In the upper plot of Fig. 1, the red markers represent the intra-macropulse beam positions reconstructed from BPM signals

* Work supported by National Natural Science Foundation of China (No. 12305166) and the Natural Science Foundation of Guangdong Province, China (No. 2024A1515010016), Xie Jialin's Grant (No. E65461U2).
† yangrenjun@ihep.ac.cn

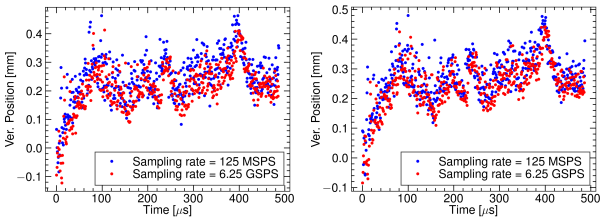

Figure 1: Comparison of intra-pulse beam position calculation results at different sampling rates with filter bandwidths of 50 MHz (upper) and 2 MHz (bottom).

sampled at 6.25 GSPS after applying a digital band-pass filter with a center frequency of 324 MHz and a bandwidth of 50 MHz. The blue markers correspond to the reconstruction results obtained by first applying the same filter to the original waveform, followed by down-sampling by a factor of 50 before the beam position calculation, corresponding to an effective sampling rate of 125 MSPS. In the lower plot of Fig. 1, the red markers show the intra-macropulse beam positions reconstructed using a digital band-pass filter centered at 324 MHz with a bandwidth of 2 MHz. The blue markers represent the reconstruction results obtained from the down-sampled waveform using a digital band-pass filter centered at 51 MHz with the same bandwidth of 2 MHz. These figures show that a sampling rate of 125 MSPS is sufficient for accurate intra-macropulse beam position measurement, while the reconstruction accuracy is not significantly affected by the selected filter bandwidth within the present measurement conditions.

EXPERIMENTAL RESULTS

The proposed method was applied to reconstruct the intra-macropulse beam position evolution using BPMs installed along the MEBT and LRBT sections of the CSNS LINAC. To reduce the impact of shot-to-shot jitter, measurements from more than 10 shots were analyzed, and the mean value together with the standard deviation was calculated for some BPMs. And all the measurements were performed using the same oscilloscope operated at a sampling rate of 1 GSPS with 16-bit vertical resolution. During the signal processing procedure, no down-sampling was applied, and the intra-macropulse beam positions were reconstructed using a digital band-pass filter with a center frequency of 324 MHz and a bandwidth of 2 MHz.The reconstructed intra-macropulse beam position evolution is shown in Fig. 2 for the LRBT section with a chopping frequency of 1.02 MHz measured in November 2025, Fig. 3 for the MEBT section with a chopping frequency of 0.51 MHz measured in April 2026, and

Fig. 4 for the LRBT section with a chopping frequency of 0.51 MHz measured in April 2026.

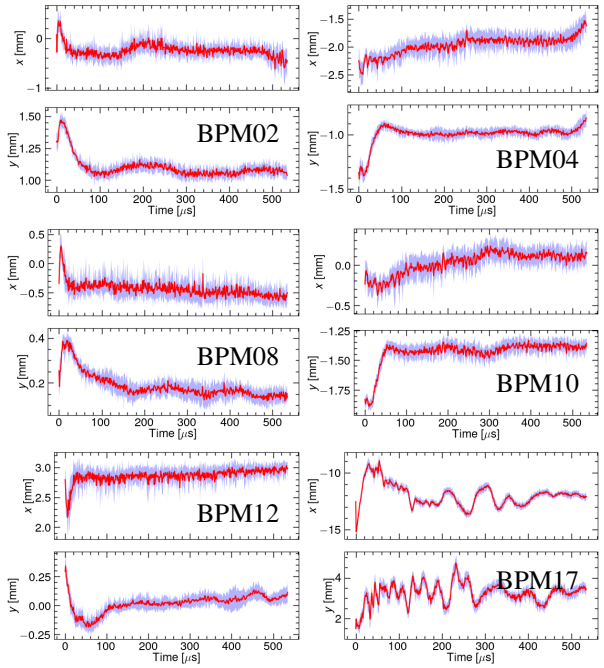

Figure 2: Observed intra-macropulse beam position oscillation in the LRBT section with a chopping frequency of 1.02 MHz (November 2025).

Table 1: Deviation of the Intra-Macropulse Beam Positions Measured in the LRBT Section (November 2025)

BPM	X (mm)	Y (mm)
LRBPM02	0.22	0.10
LRBPM04	0.24	0.09
LRBPM08	0.22	0.07
LRBPM10	0.19	0.12
LRBPM12	0.20	0.10
LRBPM17	0.31	0.35

Although the absolute beam position and the intra-macropulse jitter pattern in the LRBT section vary under different operating conditions, the measured beam position jitter remains at a comparable level for most BPMs except for LRBPM17, as summarized in Tab. 1 and Tab. 3. As shown in Tab. 2, the intra-macropulse beam position jitter in the MEBT section is generally smaller than that observed in the LRBT section, while the jitter in the vertical direction is significantly lower than that in the horizontal direction.

A common feature observed in all measurements is that the beam head exhibits significantly larger position fluctuations than the pulse tail. In particular, the peak-to-peak beam position variation at the beginning of the macro-pulse exceeds 5 mm in several BPMs, while the fluctuation amplitude gradually decreases along the pulse and eventually approaches a quasi-steady state. In the LRBT section, pronounced beam head fluctuations are observed in both the horizontal and vertical directions for most BPM locations.

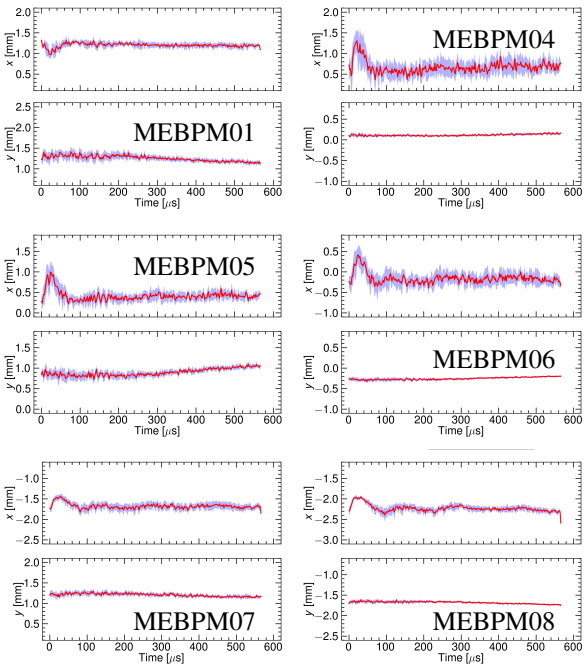

Figure 3: Observed intra-macropulse beam position oscillation in the MEBT section with a chopping frequency of 0.51 MHz (April 2026).

Table 2: Deviation of the Intra-Macropulse Beam Positions Measured in the MEBT Section (April 2026)

BPM	X (mm)	Y (mm)
MEBTBPM01	0.05	0.07
MEBTBPM04	0.14	0.02
MEBTBPM05	0.10	0.08
MEBTBPM06	0.13	0.03
MEBTBPM07	0.06	0.04
MEBTBPM08	0.08	0.03

The fluctuation amplitude ranges from approximately 1 mm to 5 mm, and the transient duration exceeds 100 μs. In contrast, the beam head fluctuation observed in the MEBT section is generally smaller than 1 mm, with a transient duration shorter than 85 μs.

Table 3: Deviation of the Intra-Macropulse Beam Positions Measured in the LRBT Section with a Chopping Frequency of 0.51 MHz (April 2026)

BPM	X (mm)	Y (mm)
LRBPM02	0.19	0.19
LRBPM04	0.19	0.19
LRBPM08	0.23	0.07
LRBPM10	0.19	0.13
LRBPM12	0.18	0.14
LRBPM17	2.98	1.24

In addition to the BPM measurements, a similar transient behavior at the macro-pulse head was also observed in the laser wire prototype at the LRBT (near LRBPM14) [1]. Fig-

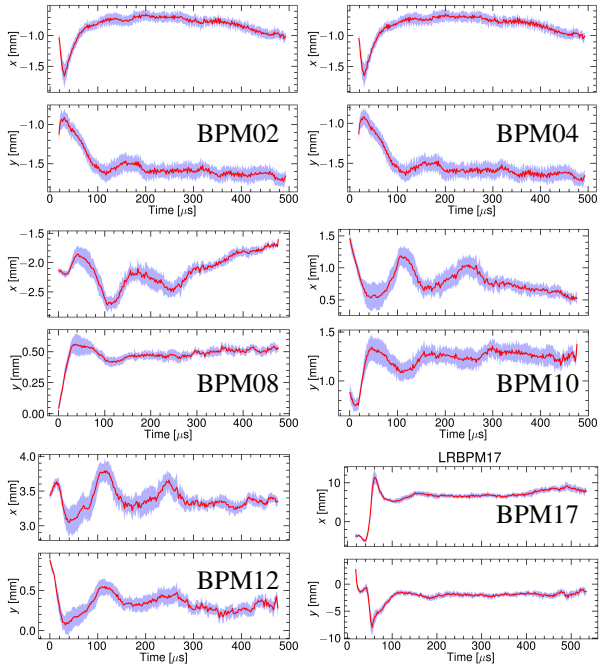

Figure 4: Observed intra-macropulse beam position oscillation in the LRBT section with a chopping frequency of 0.51 MHz (April 2026).

ure 5 shows the evolution of the beam position and beam size measured by the laser wire system as a function of the delay time within the macro-pulse. A clear beam position variation of approximately 0.5 mm is observed during the first ~ 60 μs of the pulse, while the beam size exhibits a similar transient evolution. These measurements additional confirmed the intra-macropulse beam position drift at the first 100 μs.

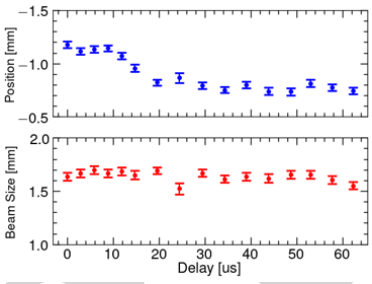

Figure 5: Temporal evolution of the beam position and beam size measured by the laser wire system within the macro-pulse.

A correlation is observed between the beam position jitter and the intra-macropulse beam position drift. In general, larger jitter appears at locations where the beam position shows stronger transient drift or larger deviation from the steady-state orbit. As an example, Fig. 6 shows the horizontal and vertical jitter waveforms measured at MEBTBPM05 and LRBPM06 (April 2026).

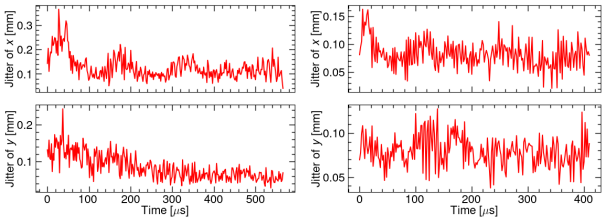

Figure 6: Shot-to-shot intra-macropulse beam position jitter measured at MEBPM05 (upper) and LRBPM04 (April 2026) (bottom).

DISCUSSION

The consistent observation of enhanced beam head fluctuations in different LINAC sections and independent diagnostics suggests that the phenomenon is related to the transient beam dynamics during the initial stage of the macro-pulse. One possible explanation is the build-up process of space charge compensation (SCC) in the low-energy transport section (LEBT) where the H^- beam energy is 50 keV [2, 3].

For intense low-energy H^- beams, the interaction between the beam and the residual gas produces secondary charged particles, which partially compensate the beam space charge field. However, the SCC process requires a finite build-up time before reaching equilibrium. The pulsed beam may experience significant mismatch and instability during the initial uncompensated stage of the pulse, while the beam transport gradually approaches steady-state conditions after the SCC equilibrium is established. The SCC build-up time can be approximated through [4]

$$\tau = \frac{\eta}{n_g \sigma(E_b) v_b}, \quad (1)$$

where η is the SCC degree, n_g is the residual gas density, $\sigma(E_b)$ is the ionization cross section, and v_b is the beam velocity. Assuming a residual gas pressure of 1×10^{-3} Pa, an SCC degree of $\eta = 0.9$, and an ionization cross section of approximately 2×10^{-20} m^2 for H^- beam energy at the LEBT section. The estimated SCC build-up time of approximately 60 μs is roughly consistent with the experimentally observed transient duration at the macro-pulse head.

The observations at CSNS exhibit comparable temporal characteristics, especially during the first tens of microseconds of the macro-pulse. Although the present results suggest a possible correlation between the observed beam head fluctuation and the SCC build-up process, the detailed physical mechanism has not yet been fully understood. Further investigations will therefore be carried out under different beam intensities, chopping patterns, and vacuum conditions, together with additional beam dynamics simulations and diagnostic measurements, to better understand the origin of the observed intra-macropulse beam fluctuations.

REFERENCES

[1] B. Zhang *et al.*, "A prototype of a non-invasive laser wire beam profile monitor for the negative hydrogen beam at the CSNS LINAC", *Nucl. Instrum. Methods Phys. Res. Sec. A*, vol. 1087, p. 171429, 2026. doi:10.1016/j.nima.2026.171429

[2] S. Artikova and P. Address, "Space Charge Neutralization Studies with H- Beam in Low Energy Beam Transport Test Stand", in *Proc. IPAC'16*, Busan, Korea, Jun. 2016, pp. 677–679. doi:10.18429/JACoW-IPAC2016-MOPOR035

[3] W. Chen *et al.*, "Operation of RF-driven negative hydrogen ion source in China Spallation Neutron Source", *Rev. Sci. Instrum.*, vol. 90, no. 11, p. 113320, Nov. 2019. doi:10.1063/1.5128553

[4] E. Flannigan *et al.*, "A review of space charge compensation diagnostics", in *Proc. IBIC'25*, Liverpool, UK, Sep. 2025, pp. 328–334. doi:10.18429/JACoW-IBIC2025-TUDI01

[5] J. Wei *et al.*, "China Spallation Neutron Source: Design, R&D, and outlook", *Nucl. Instrum. Methods Phys. Res. A*, vol. 600, pp. 10–13, 2009. doi:10.1016/j.nima.2008.11.017

[6] S. Wang *et al.*, "Introduction to the overall physics design of CSNS accelerators", *Chin. Phys. C*, vol. 33, p. 1, 2009. doi:10.1088/1674-1137/33/S2/001

[7] M. A. Rehman *et al.*, "Development and operation of shorted stripline bpm system for the csns linac", *Nucl. Instrum. Methods Phys. Res. Sec. A*, vol. 1080, p. 170671, 2025. doi:10.1016/j.nima.2025.170671

[8] A. Riazantsev *et al.*, "Digital signal processing techniques for beam position monitors", *J. Instrum.*, vol. 11, T03002, 2016. doi:10.1088/1748-0221/11/03/T03002

[9] A. Reiter and R. Singh, "Comparison of beam position calculation methods for application in digital acquisition systems", *Nucl. Instrum. Methods Phys. Res. A*, vol. 890, pp. 18–27, 2018. doi:10.1016/j.nima.2018.02.046